A reexamination of the S0→S1 excitation spectrum of dimethylaniline

Robert A. Weersink, Stephen C. Wallace, and Robert D. Gordon

Citation: The Journal of Chemical Physics **103**, 9530 (1995); doi: 10.1063/1.469967
View online: http://dx.doi.org/10.1063/1.469967
View Table of Contents: http://scitation.aip.org/content/aip/journal/jcp/103/22?ver=pdfcov
Published by the AIP Publishing

A re-examination of the $S_0 \rightarrow S_1$ excitation spectrum of dimethylaniline

Robert A. Weersink and Stephen C. Wallace
Department of Chemistry, University of Toronto M5S 1A1, Canada

Robert D. Gordon
Department of Chemistry, Queen's University, Kingston K7L 3N6, Canada

(Received 11 May 1995, accepted 6 September 1995)

A new assignment for the $S_0 \rightarrow S_1$ transition of N,N-dimethylaniline (DMA) and related derivatives is presented. The low frequency bands and long Franck–Condon envelope observed in DMA-h_6 and DMA-d_6 are assigned to the coupled methyl torsion mode of the amino group, not to torsion of the amino substituent about the C–N bond. This new assignment is consistent with the change in frequency of the excitation bands upon deuteration of the methyl groups and the strong origin transitions observed in the excitation spectra of other alkyl anilines. The assignment was confirmed by simulations of the excitation spectra of DMA-h_6 and DMA-d_6, with parameters of the calculated potential energy surface determined to be $V_3 = 148.0 \pm 0.5$ cm^{-1}, $V_+ = -31.6 \pm 0.5$ cm^{-1}, $V_- = 8.5 \pm 0.5$ cm^{-1}, and $V_6 = -15 \pm 0.5$ cm^{-1}. By Franck–Condon analysis, it was determined that the weak origin transition is due to the shifting of the S_1 torsion minimum by 40° along the gearing coordinate relative to the corresponding minimum in the ground state.

I. INTRODUCTION

The twisted intramolecular charge transfer process (TICT) model requires a twisting of the donor group by 90° relative to the acceptor group to stabilize the charge transfer state.[1] In derivatives of dimethylaniline (DMA), such as dimethylamino benzonitrile (DMABN), the donor group is the dimethylamino group and the acceptor group is a benzene ring substituted in the *para* position. Because of the twisting motion, there has been considerable interest in determining the correct potential energy surface along this coordinate for the S_0, ^1L_b, and ^1L_a electronic states. There is much evidence in the literature supporting a TICT process in solution, where solvation must play a role in stabilizing the twisted state.

This study aims to examine the situation in the gas phase. Several studies of DMA and DMABN cooled in a supersonic jet expansion have been done to elucidate information regarding the excited state potential energy surfaces, since such a preparation removes much of the spectral congestion observed in the condensed phase. The observed spectra exhibit a weak origin and long Franck–Condon progression, with a large number of low frequency vibrational bands. A jet-cooled REMPI study of DMABN and DMA assigned the observed low frequency modes in the $S_0 \rightarrow S_1$ spectrum to inversion and torsion of the whole dimethyl amino substituent about the $C_{aryl}-N$ bond.[2] Based on a Franck–Condon analysis, the authors concluded that the minimum energy configuration of the amino group in DMA and DMABN is twisted by about 30° in the S_1 state relative to the minimum energy configuration of the S_0 state. The assumed symmetry of the torsion potential, however, is incorrect since it neglects the plane of symmetry along the long axis of the molecule. By assuming the amino group is twisted out of the plane by 30°, the potential is antisymmetric with respect to the vertical plane of symmetry along the long axis of the molecule.

A subsequent analysis[3] of the same data again assigned the bands to dimethylamino torsion, deriving a S_1 potential energy surface that exhibited the proper symmetry and accurately fit several of the observed energies and intensities of the observed DMA bands. The calculated PES has minima at $\pm 25°$ relative to the planar configuration of the ground electronic state. The model, however, ignores several bands and has difficulties in predicting the observed excitation spectrum of DMABN with the methyl groups deuterated, DMABN-d_6.[2]

A moderately high resolution band contour analysis of DMABN prepared in a jet expansion[4] concluded that the amino group is twisted from the planar position by about 30° in the S_1 state, with the potential having a double-minimum character. The estimate of the twist angle had a high uncertainty since the calculated spectra were rather insensitive to the dimethylamino torsion coordinate, indicating to the authors that the barrier to amino torsion about the planar position was either very small or non-existent.

The conformation of the amino substituent in aniline derivatives depends on the electronic properties of the nitrogen. Its hybridization and conjugation with the benzene ring determine the potential energy surfaces for the amino torsion and the inversion motions. In the ground electronic state, the nitrogen is basically of sp^3 hybridization,[5–7] as evidenced by the pyramidal structure of the amino group. The lone pair of electrons on the nitrogen in the sp^3 hybrid form can undergo conjugation with the π electrons of the benzene ring. Therefore, the C_{aryl}–N bond is not exclusively a σ bond, but it has some π character as well. Because the nitrogen is essentially sp^3 hybridized, the substituents attached to the end of the nitrogen are out-of-plane with respect to the benzene plane.

Torsion about the C_{aryl}–N bond, however, is not the only possible large amplitude vibration in the dimethylamino substituent. Inversion of the CNC plane of the substituent through the plane of the benzene ring is also expected to occur. In aniline, this mode is prominent in the excitation and

 0021-9606/95/103(22)/9530/11/$6.00

emission spectra.[5–8] As in aniline, an inversion barrier exists at the planar position in the S_0 state. Microwave studies of DMA (Ref. 9) indicate a pyramidal conformation in S_0 with the C_{aryl}–N bond making an angle of about 27° with the Me-N-Me plane, and a barrier to inversion on the order of 250 cm^{-1}. For the S_1 state, it has been determined that along the inversion coordinate, the minimum occurs at the planar position.[4] As well, torsion of the methyl rotors can occur. Since the two rotors are sterically close together, it is expected that the motion of the rotors are coupled.[10–13] Separation of all of these large amplitude vibrations into distinct modes may, in fact, be impossible, since the potential energy surface for one vibration is influenced by the position that the molecule is situated along the potential energy surface of one of the other vibrations.

This paper presents a new analysis of the $S_0 \rightarrow S_1$ spectra of DMA and DMABN, assigning the observed bands to the coupled methyl torsion mode of the dimethylamino substituent. This analysis is consistent with both the observed shift of the $S_0 \rightarrow S_1$ spectrum of DMA-d_6, and with the excitation spectra of other alkyl anilines. It is found that there is a moderate barrier to complete internal rotation of the rotors, with a small degree of coupling between the rotors. Also, the minimum energy configurations of the rotors shift dramatically in the excited state relative to similar configurations in the ground state, likely the result of coupling of the methyl torsion modes with the inversion mode in the S_0 state.

II. EXPERIMENT

Details of the experimental setup have been described previously.[14,15] Therefore, only a brief discussion of the expansion conditions and the excitation sources for the multiphoton ionization and fluorescence emission experiments will be given.

The molecule was prepared in a continuous free-jet expansion with He as the carrier gas. The nozzle was fitted with a circular pinhole of diameter 25, 50, or 100 μm and heated to about 50-75 °C to increase the concentration of DMA in the expansion. The backing pressure was typically between 0.5 and 5 atm. DMA was used (Aldrich 99+%) without further purification. DMA-d_6 was prepared by reacting aniline with ethylchloroformate to make the required amide which was subsequently reduced with $LiAlD_4$ to make NMA-d_3. The procedure was repeated once to make DMA-d_6.[16]

Excitation spectra of the lowest excited state of the isolated DMA were acquired using 2-color, 1+1 resonance enhanced multiphoton ionization (REMPI). The doubled output of a Nd:YAG laser (Spectra-Physics GCR-3), Q-switched at a repetition rate of 10 Hz, was split to pump two dye lasers (Quanta-Ray PDL). The output of these lasers was then doubled with a 2 cm long KDP crystal to give pulsed ultraviolet light of 5-7 ns duration, 0.5 cm^{-1} linewidth, and a pulse energy of 5 mJ. Either a Quanta-Ray WEX (Wavelength Extender), or a home-built computer-controlled tracking system was used to maintain the phase matching angle of the doubling crystals while the dye lasers were being scanned. Temporal overlap between the two pulses was achieved though a delay line in the path of λ_2. Both ultraviolet beams were directed 3-5 mm in front of the nozzle, and collimated to form a spot size of approximately 5 mm in diameter on the jet axis. To avoid saturation of the excitation transition and to maximize the ratio of two-colour to the one-colour signal of λ_1 alone, the intensity of λ_1 was attenuated either by neutral density filters or with a variable attenuator.

The ions produced in the expansion were deflected into a quadrupole mass spectrometer (VG QXK300) where they were detected and analyzed. When no mass resolution was required, the mass spectrometer was left off. Details of the ion extraction configuration and mass spectrometer are described in a previous publication.[14]

Dispersed fluorescence emission data were collected using the time-correlated-single-photon counting method (TCSPC). The second harmonic of a cw mode-locked Nd:YAG laser (Spectra Physics 3460 laser, Spectra Physics 342A mode-locker) synchronously-pumped a tunable, extended cavity dye laser (Spectra Physics 375B), with an acousto-optic cavity dumper (Spectra Physics 344) operating at 4.1 MHz. Rh6G was used in the dye laser with an average power of 300 mW at 603 nm. This output was doubled in a 1 cm^3 $LiIO_3$ crystal to produce 15-30 mW of UV light, for a pulse energy of 3-5 nJ. This excitation beam, focused to a 100 μm waist crossed the jet axis at right angles, 20-30 nozzle diameters downstream from the pinhole. Light from the fluorescing region of the jet was collected on the axis mutually perpendicular to that of the laser beam and the jet axis and focused into the entrance slit of a monochromator (GCA McPherson 0.35 m, f/6.5). The dispersed fluorescence which exits the monochromator is detected by a photomultiplier tube (Hamamtsu R1527). Details of the TCSPC electronics are given in a previous publication.[15]

III. RESULTS

A. Excitation Spectra of DMA

The excitation spectra of DMA-h_6 and DMA-d_6 are depicted in Figure 1. The spectrum of DMA-h_6 is very similar to that previously reported.[2] The lowest energy transition is the weak band observed at 32 895.8 cm^{-1}. Examination of the region below this band found no evidence for any other transitions and the relative intensities of the observed bands did not change under a variety of expansion conditions. Therefore, the weak band at 32 895.8 cm^{-1} is assigned to the origin transition. This assignment is consistent with previous assignments of DMA and DMABN.[2] Prominent bands occur at 70, 100, 130, and 165 cm^{-1} above the origin transition, with a weaker band occuring at 118 cm^{-1}. Large changes in the intensities and frequencies are observed in the excitation spectrum of DMA-d_6 (Figure 1b). The origin of DMA-d_6 is at 32 976.7 cm^{-1}, higher in energy than the origin of DMA-h_6. Such a blue shift indicates that the modes involving the deuterated atoms have a higher zero-point energy in S_0 than in S_1. The band positions are very similar to those in the excitation spectrum of DMABN-d_6 (Ref. 2) but differences occur in the intensities of some of the bands. This may be the result of saturation in the excitation spectrum of DMA-d_6, which will increase the relative intensities of the weaker bands. Since only a small amount of DMA-d_6 sample was

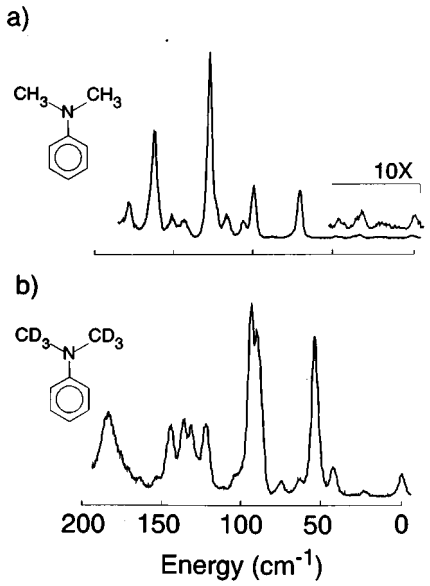

FIG. 1. 2-Color resonance enhanced multiphoton ionization spectrum of the S_1 state of (a) DMA-h_6 and (b) DMA-d_6. The weak origins occur at 32 895.8 cm^{-1} and 32 976.7 cm^{-1} for DMA-h_6 and DMA-d_6, respectively.

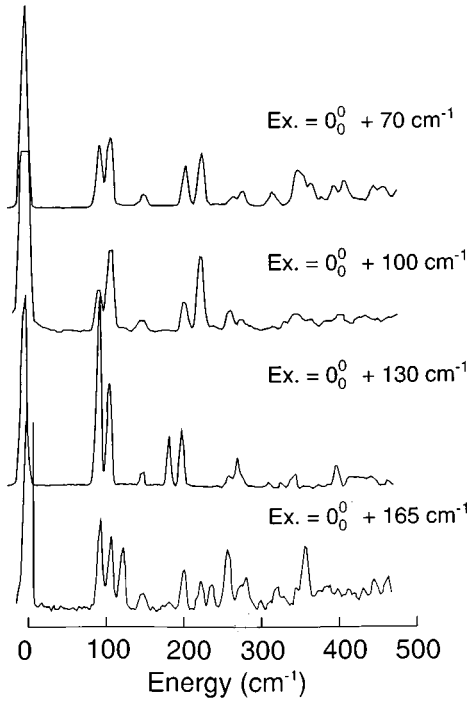

FIG. 2. Single vibronic fluorescence emission spectra following excitation of various bands in the DMA excitation spectrum.

available, the regular tests for saturation were sacrificed in favour of obtaining the correct band positions. It has been postulated that the origin of the DMA-d_6 spectrum is not observed.[3] To tests this hypothesis, the region to lower energy of the band at 32 976.7 cm^{-1} was examined carefully for any other weak transitions. None were observed and therefore the assignment of the band at 32 976.7 cm^{-1} to the origin transition is made with confidence. The large changes in frequency of the S_1 bands indicates that the large amplitude motion in the excited state that gives rise to these low frequency bands must be strongly affected by the change in mass of the substituent. The mode most consistent with this large change in frequency is methyl torsion.

B. Emission spectra of DMA

Single vibronic level fluorescence emission spectra of DMA-h_6 excited at a number of S_1 bands are depicted in Figure 2. The emission spectra resulting from excitation of most of the noted bands in Figure 2 all have similar low frequency bands while the 118 cm^{-1} band has a different emission spectrum. The similarities in the emission spectra indicate that the 70, 100, 130, and 165 cm^{-1} bands of the excitation spectrum belong to the same progression. Any model used to predict the the excitation spectrum of DMA must therefore include these bands.

The single vibronic level fluorescence emission spectra of DMA-h_6 and DMA- d_6 excited at their respective strongest transitions are compared in Figure 3. Emission bands below 300 cm^{-1} do not show a large deuteration shift and are therefore unlikely to involve methyl torsion. Thus the expected methyl torsion bands are likely to fall in the crowded higher-energy region. Consequently, torsional frequencies, and hence the barrier to internal rotation are significantly higher in S_0 than in S_1. This is supported by the abscence of torsion splittings in the microwave spectrum of DMA (Ref. 9) and by the fact that dimethylamine has a barrier to internal roation of about 1280 cm^{-1}.[18] The higher barrier in S_0 is also consistent with the observed blue shift in the origin of the excitation spectrum of DMA-d_6 relative to the origin of DMA-h_6. The small shifts in the frequencies of the lowest emission bands signify that the mode giving

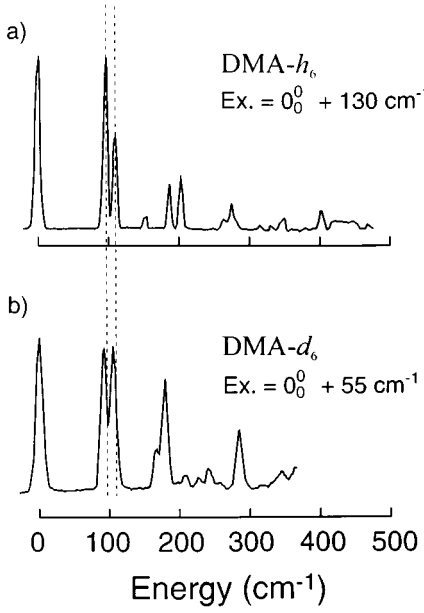

FIG. 3. Single vibronic fluorescence emission spectra following excitation of the strongest bands in the excitation spectra of DMA-h_6 and DMA-d_6.

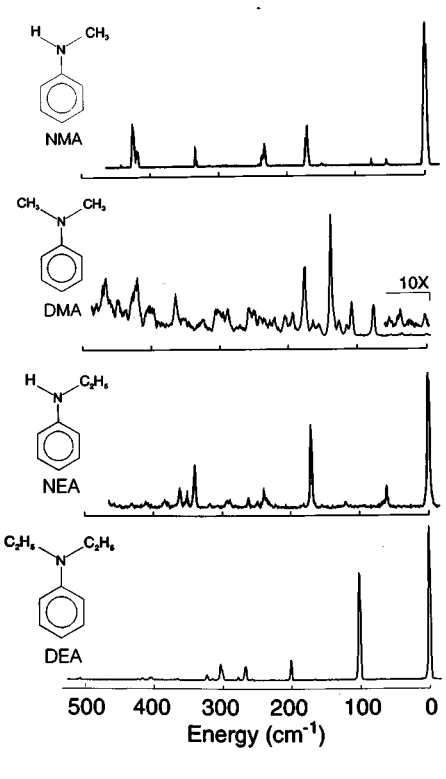

FIG. 4. 2-Color resonance enhanced multiphoton ionization spectrum of the S_1 states of (a) NMA, (b) DMA-h_6, (c) NEA, (d) DEA. The origins occur at 33 302.4, 32 895.8 cm^{-1}, 33 281.7, and 32 294.5 cm^{-1}, respectively.

rise to these bands is minimally affected by the deuteration of the methyl groups, and is therefore likely either the amino torsion mode and/or the inversion mode of the amino group. Congestion in the spectra above 300 cm^{-1} makes it difficult to assign those bands in this region that are the result of methyl torsion.

C. Excitation spectra of other alkyl anilines

The excitation spectra of DMA and other alkyl anilines, N-methylaniline (NMA), N-ethylaniline (NEA) and diethylaniline (DEA) are shown in Figure 4. In contrast to DMA, the other alkyl anilines have strong origin transitions. The origins of the S_1 states of NMA, NEA, and DEA occur at 33 302.4, 33 281.7, and 32 294.5 cm^{-1} respectively. These alkyl anilines have only a few low frequency bands that are weak in intensity. In contrast, DMA has many strong low frequency bands. Consequently, the low frequency modes and Franck–Condon envelope of DMA must be due to a mode that is not found in NMA, NEA, or DEA. Another pair of compounds that are useful comparative references are N,N-pyrrolidinobenzonitrile (PYRBN) and ethyl, N,N-pyrrolidinobenzoate (PYRBEE). The excitation spectra of the $S_0 \rightarrow S_1$ transition of PYRBN and PYRBEE also exhibit a strong origin transition with a few very weak low frequency transitions.[17]

Consideration of the possible large amplitude, low frequency modes of the alkylamino group of these alkyl anlines suggests that the long Franck–Condon progression and low frequency bands observed in the DMA spectrum are the result of methyl torsion. The potential energy surface of the amino torsion in all five alkyl anilines should be approximately equivalent. The steric interactions of the alkyl groups with the benzene ring should be the same for DMA, DEA and PYRBEE. Therefore, one should expect the same Franck–Condon envelope for the progression of this mode in the $S_0 \rightarrow S_1$ spectra of these alkyl anilines, although differences in the masses of the substituent would affect the vibrational frequencies. The inversion potential may vary from molecule to molecule, but the S_1 state should be essentially planar with a flat well as in aniline. Hence, the observed progression should have similar Franck–Condon envelopes for the progression of the inversion mode in the vibronic spectra of these anilines. Only the alkyl torsion mode will be different in all molecules and can be expected to result in differences in the observed excitation spectra. From these comparisons, it can be inferred that the weak origin transition and low frequency transitions are due to the methyl torsion mode.

The only assignment of the the DMA excitation spectrum that is consistent with the deuteration data and the comparisons made between the excitation spectra of DMA and other alkyl anilines is that of the coupled methyl rotor modes of the dimethylamino group. To confirm this assignment, simulations of the excitation spectra of DMA-h_6 and DMA-d_6 were carried out.

IV. HAMILTONIAN FOR COUPLED METHYL ROTORS

Swalen and Costain were the first to study the problem of two internal methyl rotors as a means of assigning the vibrational spectra of acetone.[10,11,19,20] The theory has been expanded and applied to a large number of molecules with two internal rotors.[12,13,21,22]

The correct form of the coupled methyl rotor potential is determined by the symmetry of the molecule. For DMA, the symmetries of the ground and excited states are different because of differences in the out-of-plane bending mode of the amino group in each electronic state. For the ground state, the minimum energy configuration is with the amino group bent out of the plane of the benzene ring. Using the notation of Durig,[13] the molecule can be described as $C_{3v}T-C_SF-C_{3v}T$, indicating that the two equivalent rotors are of C_{3v} symmetry attached to frame of C_S symmetry. The correct symmetry of the potential energy surface for the coupled methyl rotors in the ground state is therefore G_{18}. This means that the motion of the two rotors must be symmetric with respect to the plane of symmetry perpendicular to the plane of the benzene ring. Therefore, the gearing mode is symmetric and the anti-gearing mode is antisymmetric. The only restriction placed on the minimum energy configuration of the rotors is that they retain the mirror symmetry required by the C_S point group.

In the excited state, the amino group is planar with respect to the plane of the benzene ring, and therefore the frame has C_{2v} symmetry. Therefore the double rotor potential energy surface has G_{36} symmetry, placing further restrictions on the minimum energy configurations of the potential energy surface. With a C_{2v} frame the rotors must be symmetric with respect to the vertical and horizontal planes of

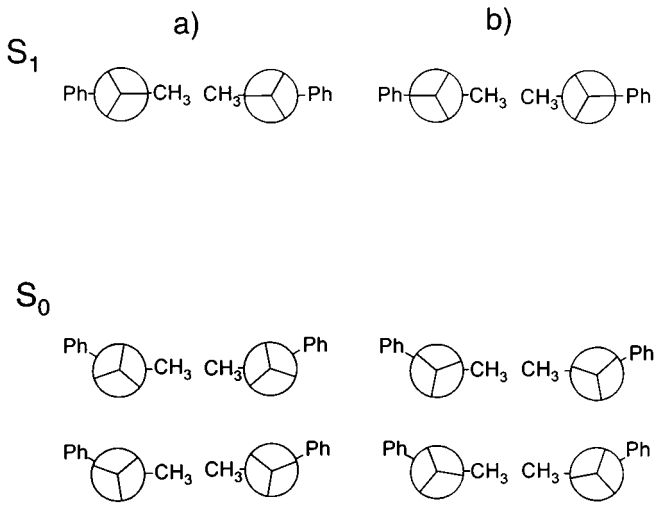

FIG. 5. Newman projections, looking down the CH_3-N bonds, of the possible conformations of DMA. The CH_3-N-CH_3 plane is horizontal, with torsion angles measured from the horizontal plane. In the planar S_1 conformation, the methyl groups must stagger (a) or eclipse (b) the C_{aryl}–N bond. In S_0, the C_{aryl}–N bond is approximately 27° out of the plane of the horizontal plane, and the methyl torsional angles are displaced 40° in the same (top row of S_0 conformations) or the opposite (bottom row of S_0 conformations) direction from the C_{aryl}–N bond.

symmetry. Therefore, there can only be two possible minimum energy configurations, as depicted in Figure 5; with each methyl rotor staggered (Figure 5a) or eclipsed (Figure 5b) with respect to the benzene ring.

Since the calculations are for the S_1 state of DMA, the proposed Hamiltonian is appropriate to G_{36} symmetry.

A. Kinetic energy

The kinetic energy terms for the coupled rotor case are[10]

$$\mathbf{T}=F(\mathbf{p}_1^2+\mathbf{p}_2^2)+F'(\mathbf{p}_1\cdot\mathbf{p}_2+\mathbf{p}_2\cdot\mathbf{p}_1), \tag{1}$$

where the F is the rotation constant for the equivalent rotors, F' is the kinetic energy coupling term and $\mathbf{p}_i$ is the momentum operator for rotor i. The rotational constants are calculated using

$$F=\frac{\hbar^2}{4I_\phi}(r_z^{-1}+r_x^{-1}), \tag{2}$$

$$F'=\frac{\hbar^2}{4I_\phi}(r_z^{-1}-r_x^{-1}), \tag{3}$$

where

$$r_z=[1-(2\lambda_z^2 I_\phi/I_z)],$$

$$r_x=[1-(2\lambda_z^2 I_\phi/I_x)],$$

where I_ϕ is the moment of inertia of one internal rotor about its symmetry axis, I_z and I_x are the moments of inertia about the z and x axes of the molecule, λ_i is the direction cosine between the i^{th} axis and the axis of internal methyl rotation. The z axis is defined as the long axis of the molecule and the x axis is defined as the short axis in the plane of the benzene ring.

Standard bond lengths and angles were used to calculate the values of F and F'. Using equations 2 and 3, the values of F and F' for dimethylaniline are calculated to be $F=5.47\ \mathrm{cm}^{-1}$ and $F'=-0.06\ \mathrm{cm}^{-1}$.

B. Potential energy

The potential function for internal rotation of two interacting methyl rotors is an expansion of a Fourier series.[10,12,13] The terms present in the potential energy function are dependent on the symmetry of the molecule. For a molecule of G_{36} symmetry such as DMA in the S_1 state, the potential is

$$\begin{aligned}\mathbf{V}(\phi_1,\phi_2)=&V_3/2(2-\cos3\phi_1-\cos3\phi_2)\\&+V_+/2(1-\cos(3\phi_1+3\phi_2))\\&+V_-/2(1-\cos(3\phi_1-3\phi_2))\\&+V_6/2(2-\cos6\phi_1-\cos6\phi_2),\end{aligned} \tag{4}$$

where ϕ_1 and ϕ_2 are the two torsional angles defined so that both rotors are moving in the same direction. The first and last terms are potential functions used for two separate but equal rotors while the second and third terms result in coupling between the two rotors and are representative of the anti-gearing and gearing modes respectively.

C. Basis set and intensity

The assumed basis set for the double rotor problem is a product of two free rotor function,

$$\begin{aligned}|\Psi(\phi_1,\phi_2)\rangle&=\sum_{m_1}\sum_{m_2}a_m\cdot e^{im_1\phi_1}\cdot e^{im_2\phi_2}\\&=\sum_{m_1}\sum_{m_2}a_m|m_1,m_2\rangle,\end{aligned} \tag{5}$$

where the single m labelling the coefficient denotes a specific combination of m_1 and m_2 values. There are 4 A, 1 G, and 4 E symmetry species in the G_{36} molecular symmetry group. In the high barrier approximation, a given vibrational level is near 9-fold degenerate, with 1 A, 2 E and 1 G symmetry species. The 2 E symmetry species are doubly degenerate and the G species is quadruply degenerate. To calculate the energy levels, the matrix is divided into four blocks using the quantum numbers v_i and σ_i such that $m_i=3v_i+\sigma_i$, where v_i is an integer, and $\sigma_i=0,\pm1$, $i=1,2$. With $\sigma_1=\sigma_2=0$, the A levels are calculated. When $\sigma_i=0,\sigma_j=\pm1$, the G levels are calculated, but only one set of σ's are required since all four combinations of i and j will result in the same calculated energies. The E levels are separated into two blocks, one in which $\sigma_1=\sigma_2=\pm1$, the other in which $\sigma_1=\pm1,\sigma_2=\mp1$.

The intensities of the formally allowed progression are determined by calculating the Franck–Condon overlap of the two torsion-inversion levels of a transition. Symmetry requires the torsional minima in the planar S_1 to be symmetric

TABLE I. Correlation table for C_{2v} and G_{36} molecular symmetry groups with statistical weights for hydrogen nuclei in parentheses for each level.

C_{2v}	G_{36}
$A_1(28)$	$A_1(6)\oplus E_1(4)\oplus E_3(2)\oplus G(16)$
$A_2(28)$	$A_3(6)\oplus E_2(4)\oplus E_3(2)\oplus G(16)$
$B_1(36)$	$A_2(10)\oplus E_1(4)\oplus E_4(6)\oplus G(16)$
$B_2(36)$	$A_4(10)\oplus E_2(4)\oplus E_4(6)\oplus G(16)$

to the benzene plane, but there is no such restriction in pyramidal S_0. Thus an arbitrary change in the phase of the barrier is possible and must be considered. This is accomplished by introducing a phase term into the overlap calculation. If the minimum of the torsion potential energy surface undergoes a change in geometry of τ_1 and τ_2 from its ground state equilibrium position, then the overlap of two wavefunctions is then

$$\langle \Psi'(\phi_1,\phi_2)|\Psi''(\phi_1+\tau_1,\phi_2+\tau_2)\rangle$$

$$=\sum_m \sum_m a'_m a''_m \exp(-im''_1\tau_1 - im''_2\tau_2)$$

$$=\sum_m \sum_m [a'_m a''_m(\cos m_1\tau_1+\cos m_2\tau_2)+a'_m a''_m$$

$$\times(i\sin m_1\tau_1+i\sin m_2\tau_2)=G+iH, \tag{6}$$

where

$$G=\sum_m \sum_m a'_m a''_m(\cos m_1\tau_1+\cos m_2\tau_2), \tag{7}$$

$$H=\sum_m \sum_m a'_m a''_m(\sin m_1\tau_1+\sin m_2\tau_2)].$$

The intensity is then the square of the overlap,

$$I=G^2+H^2. \tag{8}$$

The values of τ_1 and τ_2 are restricted by symmetry considerations. Since the ground state is of lower symmetry, G_{18}, the only restriction placed on the values of the phase terms is that $\tau_1=-\tau_2$, consistent with motion along the symmetric gearing mode of the ground state.

In determining the calculated intensities, each level is also multiplied by the statistical weight for its respective symmetry. The correlations and statistical weights for DMA-h_6, and DMA-d_6 for each symmetry level are listed in Tables I and II.[23–25]

TABLE II. Correlation table for C_{2v} and G_{36} molecular symmetry groups with statistical weights for deuterium nuclei in parentheses for each level.

C_{2v}	G_{36}
$A_1(370)$	$A_1(66)\oplus E_1(64)\oplus E_3(64)\oplus G(176)$
$A_2(359)$	$A_3(55)\oplus E_2(72)\oplus E_3(56)\oplus G(176)$
$B_1(370)$	$A_2(66)\oplus E_1(64)\oplus E_4(64)\oplus G(176)$
$B_2(359)$	$A_4(55)\oplus E_2(72)\oplus E_4(56)\oplus G(176)$

TABLE III. Calculated torsional levels of DMA-h_6. Zero-point energy is 59.80 cm^{-1} Energies are in relative cm^{-1}. Hamiltonian parameters are $F=5.47$, $F'=-0.06$, $V_3=148.0$, $V_+=-31.6$, $V_-=8.5$, $V_6=-15.0$

	$(v_+\ v_-)$	A	G	E	E
0	(0 0)	0.00	0.67	1.34	1.34
1	(1 0)	58.90	54.51	52.48	52.41
2	(0 1)	74.40	71.06	65.38	65.47
3	(2 0)	98.95	100.22	115.00	115.85
4	(1 1)	100.80	119.75	123.30	121.76
5	(0 2)	136.88	132.41	130.26	130.92
6	(3 0)	168.40	165.15	170.01	169.19
7	(2 1)	175.59	170.86	171.02	172.30
8	(1 2)	213.24	194.77	183.91	182.60

D. Calculated excitation spectra

The calculations employed 121 basis functions in each symmetry block, consisting of eleven free rotor functions for each rotor. No change was found in the energies of the eigenfunctions when a larger basis set was used. The kinetic energy terms used in the simulation were calculated from the geometry of DMA using equations 2 and 3. The potential energy terms were varied using the Hellmann-Feynman method[26] to calculate changes in energies, until the calculated energies of the eigenfunctions matched the observed energies of the DMA-h_6 spectrum. A least squares routine was used to determine the best fit to the observed values. The calculated DMA-h_6 potential was then used in the simulation of DMA-d_6, where the only change in the Hamiltonian was the required change in the values of F and F'.

The fits were confirmed by calculating the intensities of the transitions, using equations 6, 7, and 8 and varying the values of τ_1 and τ_2 such that $\tau_1=-\tau_2$. A ground state potential energy surface of $V_3=950$ cm^{-1} was used in the intensity calculations to simulate the observed high frequency torsion modes in the emission. It was found that there was little variation in the calculated intensities with changes in the ground state potential. Confidence in the calculated intensities would increase, however, with an accurate ground state potential that included any coupling between the inversion and the torsion modes.

The kinetic energy terms were calculated from the geometry of the molecule using standard bond lengths and angles and were set at $F=5.47$ cm^{-1}, $F'=-0.06$ for DMA-h_6, $F=2.7$ cm^{-1}, $F'=-0.07$ for DMA-d_6. The potential energy parameters found to fit the observed energies best were $V_3=148.0\pm0.5$ cm^{-1}, $V_+=-31.6\pm0.5$ cm^{-1}, $V_-=8.5\pm0.5$ cm^{-1}, and $V_6=-15.0\pm0.5$ cm^{-1}. The best fit to the intensities was found with $\tau_1=-\tau_2=40°\pm2°$, a change in the minimum of the excited state potential of 40° along the gearing coordinate with respect to the ground state potential. The calculated transitions and calculated intensities for DMA-h_6 and DMA-d_6 are listed in Tables III–VI, while the calculated spectra are depicted in Figures 6 and 7.

The calculated potential energy surface is depicted in Figure 8. Two coordinates are defined along the diagonals of the plot. The anti-gearing motion is defined as $\phi_+=(\phi_1+\phi_2)/2$ and occurs along the diagonal for which

TABLE IV. Observed and calculated torsional levels and intensities of major bands of DMA-h_6. Calculated intensities with rotors twisted from S_0 position by $\pm 40°$ in a gearing motion.

Assignment G_{36}	Assignment $(\upsilon_+ \ \upsilon_-)$	Observed (cm^{-1})	Calculated (cm^{-1})	Error	Calculated Intensity
0G	(0 0)	0	0.0	0.0	0.05
2G	(0 1)	70	70.4	−0.4	0.11
3G	(2 0)	100	99.5	0.5	0.14
$5E_1$	(0 2)	130	129.6	0.3	0.19
5G	(0 2)	130	131.7	−1.7	1.00
6G	(3 0)	165	164.5	0.5	0.23
7G	(2 1)	165	170.2	−5.2	0.20
8G	(1 2)		193.2		0.50

TABLE VI. Observed and calculated torsional levels and intensities of major bands of DMA-d_6. Calculated intensities with rotors twisted from S_0 position by $\pm 40°$ in a gearing motion.

Assignment G_{36}	Assignment $(\upsilon_+ \ \upsilon_-)$	Observed (cm^{-1})	Calculated (cm^{-1})	Error	Calculated Intensity
0G	(0 0)	0	0.0	0.0	0.03
2G	(0 1)	55	51.0	4.0	0.11
3G	(2 0)	90	84.2	5.8	0.03
5G	(0 2)	95	97.8	−2.8	1.00
$5E_3$	(0 2)	95	98.5	−3.5	0.19
8G	(2 1)	135	136.3	−1.3	0.19
9G	(0 3)	147	145.0	−2.0	0.84

$\phi_1 = \phi_2$, or from the bottom left corner of the potential to the top right corner of the potential in Figure 8. The gearing motion is defined as $\phi_- = (\phi_1 - \phi_2)/2$ the diagonal for which $\phi_1 = -\phi_2$, or from the bottom right corner of the potential to the top left corner of the potential in Figure 8. In the calculated potential, a barrier exists along the anti-gearing and gearing coordinates of 296 cm^{-1}. These potentials are depicted in Figure 9. Notice that the well of the anti-gearing potential is flatter than the well of the gearing potential, consistent with the lower frequency of the anti-gearing fundamental band, calculated to occur at 58 cm^{-1}. The flatter well of the anti-gearing potential relative to the gearing potential is the result of lower steric interactions if the rotors move in the anti-gearing direction. In Figure 10, the rotors are rotated from the initial equilibrium conformations of the S_1 state, as depicted in Figure 5, by 30° along the anti-gearing (Figure 10a) and gearing (Figure 10b) coordinates. The steric interactions between the methyl hydrogens is lower for the rotors that have moved along the anti-gearing coordinate, i.e., the conformation depicted in Figure 10a than for the rotors that have moved along the gearing coordinate, i.e., the conformation depicted in Figure 10b.

The lower torsional levels can be labelled by torsional vibration quantum numbers υ_+ and υ_- for the antigearing and gearing modes, respectively, as shown in Tables III–VI. Each (υ_+, υ_-) level has nine degenerate components with symmetries $A+2E+G$. A progression is observed in the totally symmetric (under C_S) gearing mode, with maximum intensity at $\upsilon_-\ {}^2_0$ (the 130 cm^{-1} band), consistent with the 40° change in conformation described above. Since the anti-gearing mode is non-totally symmetric, the transition to the $\upsilon_+\ {}^1_0$ is forbidden, and is not observed. However, the $\upsilon_+\ {}^2_0$ transition (the 100 cm^{-1} band) would be allowed and is observed. At these lower energies, the agreement between calculated and observed spectra is excellent.

At higher torsional energies the υ_+/υ_- classification, and the rigid-molecule C_S symmetry on which it is based, are expected to break down. Selection rules based on G_{36} symmetry apply and for levels of G and E symmetry, transitions corresponding to all values of $\Delta\upsilon_+$ and $\Delta\upsilon_-$ are permitted. Several transitions corresponding to odd values of $\Delta\upsilon_+$ are predicted to have significant intensity and are indeed observed. The agreement between observed and calculated spectra is less good at higher energies, especially with regard to intensities. This may be due to significant interactions between coupled methyl torsion and other modes.

TABLE V. Calculated torsional levels of DMA-d_6. Zero-point energy is 53.69 cm^{-1} Hamiltonian parameters are $F=2.77$, $F'=-0.06$, $V_3=148.0$, $V_+=-31.6$, $V_-=8.5$, $V_6=-15.0$.

	$(\upsilon_+ \ \upsilon_-)$	A	G	E	E
0	(0 0)	0.00	0.05	0.11	0.11
1	(1 0)	38.08	37.71	37.36	37.36
2	(0 1)	51.62	51.07	50.49	50.49
3	(2 0)	77.37	78.07	80.00	80.05
4	(1 1)	80.78	84.20	86.67	86.58
5	(0 2)	96.89	97.87	98.57	98.64
6	(3 0)	123.03	115.72	115.65	115.09
7	(2 1)	130.39	124.52	115.84	116.35
8	(1 2)	140.33	136.38	129.00	129.02
9	(0 3)	144.93	145.06	143.00	143.03
10	(4 0)	145.59	145.34	163.22	162.88

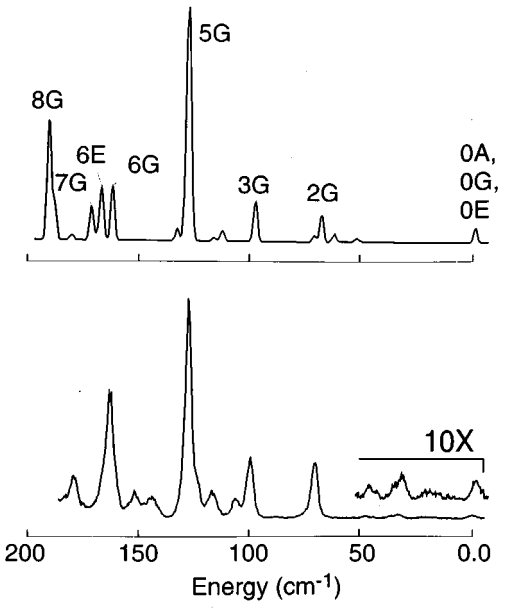

FIG. 6. Calculated (above) and observed (below) excitation spectra of DMA-h_6. The calculated Hamiltonian terms are $F=5.47$ cm^{-1}, $F'=-0.06$ cm^{-1}, $V_3=148.0$ cm^{-1}, $V_+=-31.6$ cm^{-1}, $V_-=8.5$ cm^{-1}, and $V_6=-15.0$ cm^{-1} The minimum of the potential surface is shifted by 40° along the gearing coordinate relative to the ground state potential to obtain the correct intensities.

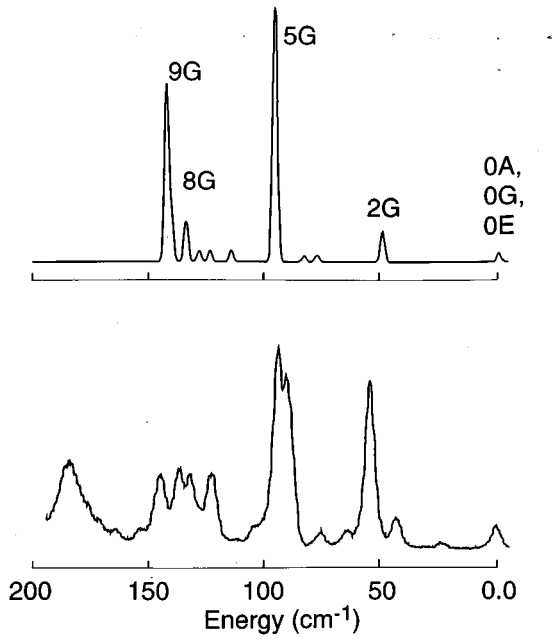

FIG. 7. Calculated (above) and observed (below) excitation spectra of DMA-d_6. The potential energy terms are identical to those used for DMA-h_6. The kinetic energy terms have been adjusted to account for the deuteration, with $F=2.77$ cm^{-1}, and $F'=-0.05$ cm^{-1}. As with the calculated DMA-h_6 spectrum, the minimum of the potential surface is shifted by 40° along the gearing coordinate to obtain the correct intensities.

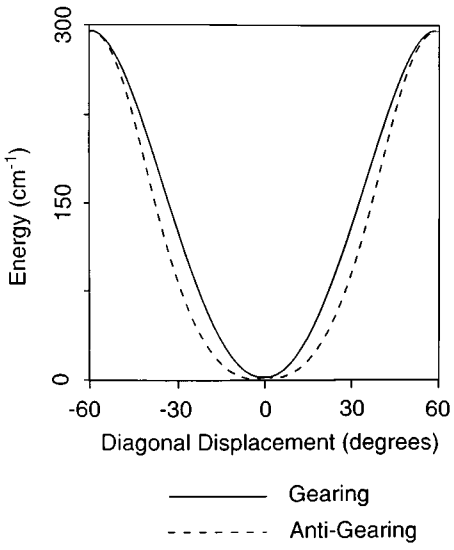

FIG. 9. Potential energy surfaces for the gearing and anti-gearing modes. The barrier to both of these modes is 296 cm^{-1}. The anti-gearing mode has a flatter potential well than the gearing mode, resulting in the fundamental of the anti-gearing mode having a lower energy than the fundamental of the gearing mode.

The low frequency bands in the emission spectra of DMA are reasonably assigned to inversion of the dimethylamino group and torsion of the whole amino group. In previous I.R studies,[27] the fundamental of the torsion of the amino group was assigned to a band at 66 cm^{-1}, approximately half the frequency of the 124 cm^{-1} band observed in the emission spectra. In the absence of torsion-inversion coupling, excitation of the S_1 torsion bands should result in similar intensity in the observed emission bands. Changes in the relative intensities of these emission bands for excitation of different S_1 torsion bands, however, indicates some coupling of the methyl torsion and inversion modes. This coupling is most likely to occur in the ground state with its double minimum potential along the inversion coordinate. With movement along the inversion coordinate, the minimum of the torsion potential changes along the gearing coordinate.

The long Franck–Condon progression has been attributed to a change in the equilibrium configurations of 40° along the gearing coordinate. This change in equilibrium configuration can be attributed primarily to activity in the S_0 state, particularly with respect to coupling between the torsion modes and the inversion mode. Consideration of the possible DMA conformations in S_0 and S_1 results in four possible paths consistent with such a change. The preferred conformation in each electronic state is determined by steric repulsion between the methyl hydrogens of the different methyl groups, steric repulsions between the methyl C–H bonds and the benzene hydrogens and electronic effects between

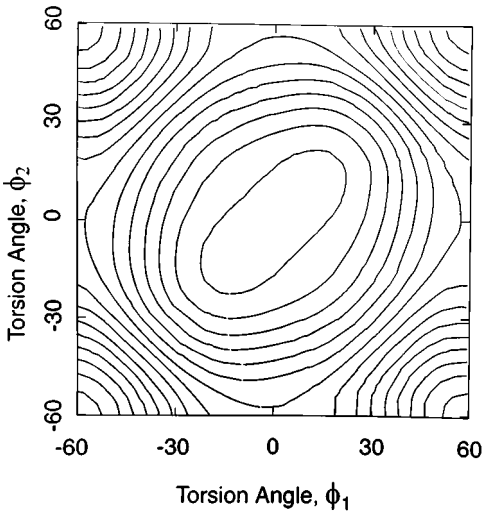

FIG. 8. Contour map of the calculated potential energy surface of DMA coupled methyl torsion mode in the S_1 state. Contour lines occur every 20 cm^{-1}. The minimum occurs at 0° along each coordinate.

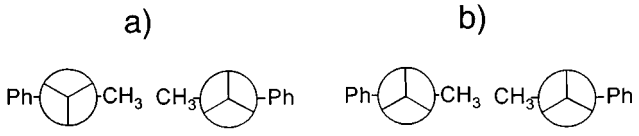

FIG. 10. Newman projections, looking down the CH_3–N bonds, of conformations of DMA after the rotors have moved from the initial equilibrium conformations by 30° along the anti-gearing coordinate (a), and the gearing coordinate (b). Steric interactions are expected to be much smaller in (a) than in (b). This is consistent with the predicted flatter well of the potential energy surface of the anti-gearing mode with respect to the potential of the gearing mode.

the C–H bonds of the methyl groups and the C_{aryl}–N bond and between the methyl C–H bonds and the neighbouring N–C_{methyl} bond.

Figure 5 depicts the staggered (a) and eclipsed (b) geometries in the S_1 state. Based on only steric effects between the rotors, DMA is likely to have a similar minimum energy configuration as the rotors in dimethylamine,[28] which has a minimum energy configuration identical to that depicted in Figure 5b, i.e. the eclipsed form. However, significant interactions occur between the methyl rotor hydrogens and benzene ring hydrogens. Calculations of the interatomic distances suggests that steric repulsions between the methyl and the benzene hydrogens are greater than steric repulstions between the two methyl groups, thereby favouring the staggered conformation (Figure 5a, top). The steric repulsion between the methyl groups and the benzene ring should be larger in S_1 than S_0 due to the shortening of the C_{aryl}–N bond from about 1.45 Å in S_0 to 1.3 Å in S_1.[4] In contrast, electronic effects favour the eclipsed form (Figure 5 b, top), since there is strong evidence indicating that methyl hydrogen bonds are attracted to the π structure of a neighbouring bond.[29] In DMA, conjugation along the C_{aryl}–N bond provides the source of attraction. In S_1, this conjugation increases as the N atom changes to an almost sp^2 hybridization, thereby increasing this electronic attraction in the S_1 state. Analogies with NMA indicate that electronic effects should favour the same equilibrium configuration in both S_0 and S_1. Electronic effects should be the principal reason for changes in the minimum energy configurations of the rotor in the different electronic states in NMA since steric interactions between the methyl group and the neighbouring amino hydrogen are small and steric interactions betwen the methyl hydrogen bonds and the benzene ring should be similar in S_0 and S_1. The strong origin transition observed in the NMA excitation spectrum (Figure 4a) indicates little change in the configuration of the rotor in S_0 and S_1 states. Therefore, the rotors in DMA would have the same configuration in S_0 and S_1 if only electronic effects were considered.

These interactions are stronger than those between the hydrogens on differing methyl groups, based on their separation distance, thereby favouring the staggered conformation (Figure 5a). A further interaction, an electronic interaction between the C–H_{methyl} bond and π electron density of the ring and the CN bond, also occurs. Recent evidence indicates that this electronic interaction favors an eclipsed form (Figure 5b), with one of the C–H_{methyl} bonds attracted to the π electron density along the CN bond. Because of these competing effects, it is difficult to know the actual preferred conformation of the methyl rotors without further experiments involving rotational resolution.

The competing strengths of the steric and electronic effects results in two possible equilibrium conformations in the S_1 state, and four in the S_0 state, as depicted in Figure 5 with four different possible transitions to account for the shift in the potential surface minima by 40° along the gearing coordinate. The differences in magnitude of the steric and electronic effects in each state is such that even if one configuration is favoured in the S_0 state, the opposing configuration may be favoured in the S_1 state, i.e. if eclipsed in S_0, staggered in S_1 . Competition between these effects also make it difficult to predict the barrier heights to complete internal rotation. An analogy may be considered with 1-methylindole,[30] in which the methyl torsion barrier is smaller in the excited state than in the ground state.

As can be seen in Figure 5, transitions between either of the possible S_0 equilibrium configurations to either the staggered or eclipsed S_1 configurations would result in a shift in the potential minima along the gearing coordinate. This shift is due to the change in orientation of the phenyl group with respect to the plane of the dimethylamino group in the S_0 and S_1 states and probable changes in the electronic interactions upon excitation. Determining the actual configurations of the excited and ground states and hence the path of the conformation change upon excitation is undeterminable from the present analysis.

V. DIMETHYLAMINO TORSIONAL MODE

Previous analysis of the low frequency bands of DMA and its derivatives, such as DMABN, has assigned these bands to torsion of the dimethylamino substituent.[2,3] Using this analysis, an S_1 potential energy surface can be derived that accurately reproduces several of the observed band energies and intensities of the observed DMA-h_6 spectrum. The model, however, ignores several bands and has difficulties in predicting the observed excitation spectrum of DMABN-d_6. To approximately fit the observed DMABN-d_6 spectrum, it was assumed that the origin transition was not observed, and that the lowest observed band was a higher frequency torsional band. As noted previously, however, the region lower in energy than the 32 976.6 cm^{-1} band of DMA-d_6 was examined carefully for other weak transitions, with none observed, and therefore this band was assigned to the origin transition.

Using the proper assignment of the origin transition of the DMA-d_6 spectrum, the torsional analysis of the dimethylamino mode should be reconsidered. Analysis of the dimethylamino torsional mode can be performed using conventional techniques.[31] The torsional potential energy surface used was of the form

$$V(\omega)=\tfrac{1}{2}V_2(1-\cos 2\theta)+\tfrac{1}{2}V_4(1-\cos 4\theta) \tag{9}$$

with the complete torsional Hamiltonian

$$-F\frac{\partial^2\Psi}{\partial\theta^2}+V(\theta)\Psi=E\Psi. \tag{10}$$

$F=\hbar/(4\pi I_m c)$ is the reduced rotational constant of the torsion mode and I_m is the reduced moment of inertia of the m^{th} top as calculated by

$$I_m=A_m\left(1-\sum_{i=1}^{3}A_m\lambda_{mi}^2/I_i\right), \tag{11}$$

where A_m is the moment of intertia of the m^{th} top about the top's axis of rotation, i represents the three principle axis of the molecule, and λ_{mi} is the direction cosine between the axis of the m^{th} top and the i^{th} principal axis. Using standard bond lengths and angles, for the dimethylamino torsion mode, $F=0.50$ cm^{-1} for DMA-h_6 and $F=0.42$ cm^{-1} for

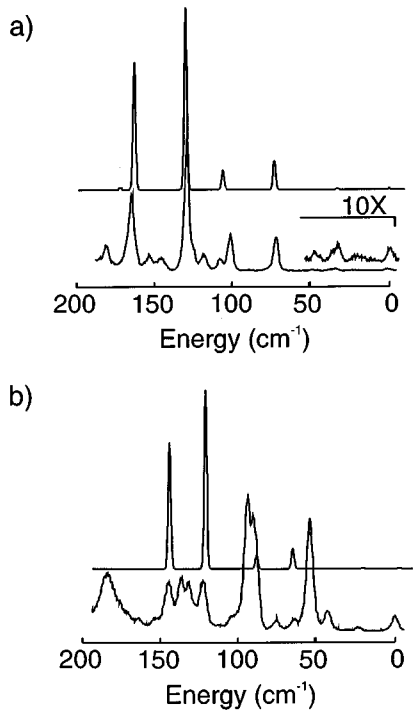

FIG. 11. Calculated and observed excitation spectra of a) DMA-h_6 and b) DMA-d_6 using the dimethylamino torsional model. The calculated potential energy surface is $V_2=3706$ cm^{-1} and $V_4=-1443$ cm^{-1} with $F=0.50$ cm^{-1} for DMA-h_6 and $F=0.42$ cm^{-1} for DMA-d_6. The calculated excitation spectrum is good for DMA-h_6 (a). However, the calculated excitation spectrum is a poor fit to the observed spectrum of DMA-d_6 (b).

DMA-d_6.[3] The best fit to the DMA-h_6 excitation spectrum is with $V_2=3706$ cm^{-1} and $V_4=-1443$ cm^{-1}.[3] This produces a double well potential centered about the $\theta=0°$ position and with minima at $\theta=\pm 25°$. The calculated excitation spectrum of DMA-h_6 is compared with the observed in Figure 11a. Transition intensities were calculated by using a simple V_2 torsion potential in the S_0 state and calculating the Franck–Condon overlap between the ground and excited state wavefunctions. All the calculated excitation transitions originated in the lowest vibrationless level of S_0. The size of the barrier in the ground state had little effect on the calculated transition intensities.

The calculated excitation spectrum of DMA-d_6 using the same potential energy parameters as above but with $F=0.42$ cm^{-1} is depicted and compared with the observed DMA-d_6 excitation spectrum in Figure 11b. In this calculation, the lowest observed transition is assigned to the origin band. The fit to the observed spectrum is poor, indicating that assignment of the low frequency bands to the dimethylamino torsional mode is not consistent with the observed isotope effect on the excitation spectra.

VI. CONCLUSION

The spectroscopy of the $S_1\rightarrow S_0$ transition of dimethylaniline is re-examined, with a new assignment for the observed low frequency bands. The observed bands in the excitation spectra of DMA and DMA- d_6 are assigned to torsion of the methyl rotors of the dimethylamino substituent, not to torsion of the amino substituent about the C–N bond. Unlike the previous assignment, this new assignment is consistent with the change in frequency of the excitation bands upon deuteration of the methyl groups and the strong origin transitions observed in the excitation spectra of other alkyl anilines. The assignment was confirmed by a simulation of the excitation spectra of DMA-h_6 and DMA-d_6.

A potential energy surface for the coupled methyl torsion modes in S_1 was determined by fitting the potential to the observed frequencies and intensities. The methyl rotors were found to be coupled with the calculated torsion parameters determined to be $V_3=148.0\pm 0.5$ cm^{-1}, $V_+=-31.6\pm 0.5$ cm^{-1}, $V_-=8.5\pm 0.5$ cm^{-1}, and $V_6=-15\pm 0.5$ cm^{-1}. As well, the weak origin of the excitation spectrum indicates that the minium energy configuration of the methyl rotors is substantially different in the excited and ground electronic states. By Franck–Condon analysis, it was determined that the minimum of the S_1 torsion potential is shifted by 40° along the gearing coordinate relative to the minimum in the ground state. It is the strong interaction of the methyl rotors with the inversion mode in the ground state which result in the broad Franck–Condon envelope in the excitation spectra of DMA-h_6 and DMA-d_6.

ACKNOWLEDGMENTS

The authors would like to acknowledge the support of the Natural Sciences and Engineering Council of Canada and CEMAID towards the completion of this work. The authors would also like to thank Professor Mark Lautens for providing the DMA-d_6.

[1] For a review, see W. Rettig, Angew. Chem. Int. Ed. Engl. **25**, 971 (1986).
[2] V. H. Grassian, J. A. Warren, E. R. Bernstein, and H. V. Secor, J. Chem. Phys. **90**, 3994 (1989).
[3] R. D. Gordon, J. Chem. Phys. **93**, 6908 (1990).
[4] O. Kajimoto, H. Yokoyama, Y. Oshima, and Y. Endo, Chem. Phys. Lett. **179**, 455 (1991).
[5] J. C. D. Brand, D. R. Williams, and T. J. Cook, J. Mol. Spectrosc. **20**, 359 (1966).
[6] M. Quack and M. Stockburger, J. Mol. Spectrosc. **43**, 87 (1972).
[7] D. A. Chernoff and S. A. Rice, J. Chem. Phys. **70**, 2511 (1979).
[8] R. D. Gordon, D. Clark, J. Crawley, and R. Mitchell, Spectrochem. Acta **40A**, 657 (1984).
[9] R. Cervellati, A. Dal Borgo, and D. G. Lister, J. Mol. Struct. **78**, 161 (1982).
[10] J. D. Swalen and C. C. Costain, J. Chem. Phys. **31**, 1562 (1959).
[11] J. S. Creighton and S. Bell, J. Mol. Spectrosc. **118**, 303 (1986).
[12] J. R. Durig, Y.S. Li and P. Groner, J. Mol. Spectrosc. **62**, 159 (1976).
[13] P. Groner and J. R. Durig, J. Chem. Phys. **66**, 1856 (1977).
[14] J. Hagar and S. C. Wallace, J. Phys. Chem. **88**, 5513 (1984).
[15] D. Demmer, G. W. Leach, E. A. Outhouse, J. W. Hagar, and S. C. Wallace, J. Phys. Chem. **94**, 582 (1990).
[16] F. Carey and R. J. Sandberg, in *Advanced Organic Chemsitry* (Plenum, New York, 1990).
[17] J. August, T. F. Palmer, J. P. Simons, C. Jouvet, and W. Rettig, Chem. Phys. Lett. **145**, 275 (1988).
[18] J.R. Durig, M. G. Griffen, and P. Groner, J. Phys. Chem. **81**, 554 (1977).
[19] R. Nelson and L. Pierce, J. Mol. Spectroc. **18**, 344 (1965).
[20] D. R. Smith, B. K. McKenna, and K. D. Moller, J. Chem. Phys. **45**, 1904 (1966).
[21] R. Engeln, J. Reuss, D. Consalvo, J. W. I. van Bladel, and A. van der Avoird, Chem. Phys. Lett. **170**, 206 (1990).

[22] X. Q. Tan, D. J. Clouthier, R. H. Judge, D. F. Plusquellic, J. L. Tomer, and D. W. Pratt, J. Chem. Phys. **95**, 7862 (1991).
[23] P. R. Bunker, *Molecular Symmetry and Spectroscopy* (Academic, New York, 1979), p. 403.
[24] J. M. Hollas, *High Resolution Spectroscopy* (Butterworths, Toronto, 1982).
[25] R. J. Myers and E. B. Wilson, J. Chem. Phys. **33**, 186 (1960).
[26] D. L. Albritton, A. L. Schemeltkopf, and R. N. Zare in *Molecular Spectroscopy: Modern Research*, edited by K.N. Rao (Academic, New York 1976), Vol. 2.
[27] C. Belorgeot, P. Quintard, P. Delorme, and V. Lorenzelli, Can. J. Spectrosc. **21**, 119 (1976).
[28] D. C. McKean, J. Chem. Phys. **79**, 2095 (1983).
[29] a) X.-Q. Tan, W. A. Majewski, D. F. Plusquellic, and D. W. Pratt, J. Chem. Phys. **94**, 7721 (1991); b) K.-Tu, F. Weinhold, and J. C. Weisshaar, *ibid*. **102**, 6787 (1995).
[30] G. A. Bickel, G. W. Leach, D. R. Demmer, J. W. Hager, and S. C. Wallace, J. Chem. Phys. **88**, 1 (1988).
[31] J. Lewis, T. Malloy, T. Chao, and J. Laane, J. Mol. Struct. **12**, 427 (1972).